Electrospray Ionization Mass Spectra of Acyl Carrier Protein are Insensitive to Its Solution Phase Conformation

Peter W. Murphy, Elden E. Rowland, and David M. Byers
Atlantic Research Centre, Department of Pediatrics, and Departments of Biochemistry and Molecular Biology, Dalhousie University, Halifax, Nova Scotia, Canada

Electrospray ionization mass spectrometry (ESI-MS) can be used to monitor conformational changes of proteins in solution based on the charge state distribution (CSD) of the corresponding gas-phase ions, although relatively few studies of acidic proteins have been reported. Here, we have compared the CSD and solution structure of recombinant *Vibrio harveyi* acyl carrier protein (rACP), a small acidic protein whose secondary and tertiary structure can be manipulated by pH, fatty acylation, and site-directed mutagenesis. Circular dichroism and intrinsic fluorescence demonstrated that apo-rACP adopts a folded helical conformation in aqueous solution below pH 6 or in 50% acetonitrile/0.1% formic acid, but is unfolded at neutral and basic pH values. A rACP mutant, in which seven conserved acidic residues were replaced with their corresponding neutral amides, was folded over the entire pH range of 5 to 9. However, under the same solvent conditions, both wild type and mutant ACPs exhibited similar CSDs (6^+–9^+ species) at all pH values. Covalent attachment of myristic acid to the phosphopantetheine prosthetic group of rACP, which is known to stabilize a folded conformation in solution, also had little influence on its CSD in either positive or negative ion modes. Overall, our results are consistent with ACP as a "natively unfolded" protein in a dynamic conformational equilibrium, which allows access to (de)protonation events during the electrospray process.   (J Am Soc Mass Spectrom 2007, 18, 1525–1532) © 2007 American Society for Mass Spectrometry

Electrospray ionization mass spectrometry (ESI-MS) has emerged as a powerful tool to investigate the conformation, dynamics, and interactions of proteins (recently reviewed in [1–5]). ESI-MS has been used to probe protein conformation in solution either by measuring mass changes in response to hydrogen-deuterium exchange, or by monitoring the charge state distribution (CSD) of protein ions in the gas-phase [6, 7]. Advantages of ESI-MS as a conformational probe include the preservation of native conformation and noncovalent protein-protein interactions, as well as its sensitivity and speed of analysis, applicability to large proteins, and compatibility with rapid mixing approaches to examine kinetic events [3]. Finally, ESI-MS can be applied to heterogeneous systems, where it has the inherent ability to detect and characterize low population conformers (such as folding intermediates), rather than merely provide an averaged signal from all the species present.

A variety of intrinsic and extrinsic factors have been shown to influence the CSD of a given protein, including its amino acid composition (i.e., potential number of ionization sites) [8] and neutralization due to proximity of opposite charges [9], as well as instrumental parameters such as curtain gas flow rate and declustering potential [10–12]. However, a dominant factor is the degree of exposure of protonation (or deprotonation) sites to the solvent [6]. Indeed, the ESI-MS average charge of native proteins from 5 to 500 kDa has recently been shown to correlate extremely well with the accessible surface area based on crystallographic data [10]. Thus, compact (i.e., folded) proteins tend to exhibit a narrow CSD with ions of lower net charge, while unfolded proteins have a broader CSD profile of higher net charge. Moreover, changes in CSD appear to be related to alterations in protein tertiary structure, rather than secondary structural changes such as helix-coil transitions [13, 14].

Both positive and negative mode ESI-MS have been used to monitor protein conformation, but Konermann and Douglas [15] have shown that correlation of CSD and pH-induced conformational changes of neutral/basic proteins such as ubiquitin, cytochrome *c* and lysozyme is only reliably observed in the positive ion mode. Relatively few studies of acidic proteins have been reported, mostly regarding metal binding acidic proteins such as calmodulin [16], calbindin [17], and iron sulfur proteins [18]. Paradoxically, calcium-induced alterations in the CSD of calmodulin were only detected in negative ion mode, while conformational change

Address reprint requests to Dr. David M. Byers, Dalhousie University/ARC, Rm. C-302 Clinical Research Centre, 5849 University Avenue, Halifax, Nova Scotia B3H 4H7, Canada. E-mail: David.Byers@Dal.ca

upon binding of trifluoperazine to Ca^{2+}-calmodulin was only seen in positive mode [16]. Clearly, caution is advised in the interpretation of CSD data and more research will be necessary to resolve these issues and extend the generality of ESI-MS as a conformational probe.

Acyl carrier protein (ACP) is a small (typically 70 to 80 residues) and acidic (pI ~ 4) protein involved in the synthesis and transfer of fatty acyl groups during the production of bacterial lipids and other specialized molecules [19]. The NMR solution structure of several ACPs reveal a highly conserved folded conformation consisting of three parallel α-helices; in acyl-ACP, these helices enclose a fatty acyl group that is covalently attached to the 4'-phosphopantetheine prosthetic group [20, 21]. Based on circular dichroism (CD) and hydrodynamic approaches, ACP from some bacterial species such as *Vibrio harveyi* is largely unfolded in solution at neutral pH, and its folded conformation can be stabilized by either fatty acylation or divalent cation binding to the acidic Helix II [22–24]. In the present study, we have manipulated recombinant *V. harveyi* ACP (rACP) to explore the relationship between CSD and higher order solution conformation as assessed by optical methods such as CD and fluorescence.

Experimental

Recombinant *Vibrio harveyi* ACP (rACP: 80 residues, average mass 8780.7 Da) was expressed and purified from a glutathione-S-transferase fusion protein as described by Flaman et al. [23]; the holo- and apo-forms of rACP (i.e., with and without phosphopantetheinylation at Ser-36) were further separated by anion-exchange (Source 15Q) chromatography [23]. Myristoyl-ACP was prepared enzymatically from holo-ACP by incubation with myristic acid (14:0), ATP, and *V. harveyi* acyl-ACP synthetase as detailed elsewhere [25]. Site-directed mutagenesis of rACP and preparation of mutant SA/SB, in which seven central conserved acidic amino acid residues are replaced with their corresponding neutral amide residues, is described in reference [26]. Similar methods were used to replace Leu at position 46 with Trp to introduce an intrinsic fluorescence probe sensitive to ACP folding (Gong and Byers, manuscript in preparation). Residue numbering corresponds to that of native *V. harveyi* ACP (SwissProt accession no. P0A2W3).

Cytochrome *c* was purchased from Pierce Biotechnology (Rockford, IL) and HPLC grade water from J. T. Baker (Phillipsburg, NJ). Formic acid was obtained from Fluka (Buchs, Switzerland) while ammonium hydroxide, acetic acid, ammonium acetate, and HPLC grade acetonitrile were all from Fisher Scientific (Fair Lawn, NJ). All chemicals were used without further purification.

Before MS analysis, solutions of apo-rACP, acyl-rACP, ACP mutants, and cytochrome *c* (1–5 μM) were exchanged using Zeba Desalt Spin columns (Pierce) into distilled H_2O and diluted into 5–10 mM ammonium acetate buffer of the desired pH values (obtained by mixing 1% solutions of ammonium hydroxide and acetic acid). Alternatively, samples were diluted into 50% acetonitrile, 0.1% formic acid. Mass spectra were recorded on an Applied Biosystems (Foster City, CA) hybrid triple quadrupole linear ion trap mass spectrometer (QTrap) equipped with a Milliliter Syringe Pump (Harvard Apparatus, Holliston, MA) and either a TurboIonspray or a Nanospray II ion source (Applied Biosystems) at a flow rate of 10 μL/min or 100 nL/min, respectively. For the Turbospray experiments, positive mode ESI spectra were recorded at an ion spray voltage of +5500 V and declustering potential (DP) of +60 V, while corresponding settings for negative mode ESI were −3000 V and −40 V, respectively. Variation of DP between 0 and 60 V did not significantly influence spectral quality or CSD in positive mode, although quality was reduced at 90 V (data not shown). Nanospray ESI spectra were recorded at an ion source voltage of +2400 V with a DP of 5 V. The sample was sprayed from a PicoTip emitter tip, distal coated fused silica 75 um i.d. with 15 um i.d. tip (New Objectives, Woburn, MA). All spectra were averaged over a minimum of 30 s and were recorded using Analyst 1.4.1 (Applied Biosystems). Average net charge was calculated from the CSD by nonlinear fitting to a Gaussian curve using GraphPadPrism 4.0 software.

For CD and intrinsic tryptophan fluorescence analysis, protein solutions (5 μM) were prepared in 10 mM ammonium acetate buffer as described above. CD spectra were recorded on a JASCO J-810 spectropolarimeter (JASCO Inc., Easton, MD) in a 1 mm path-length cuvette in a water-jacketed cell maintained at 25 °C, scanned from 190 to 260 nm in continuous mode with a speed of 20 nm/min. Fluorescence measurements were carried out on a Perkin Elmer LS50B Luminescence Spectrometer in a Perkin Elmer 10 mm quartz cell at 25 °C, with excitation at 296 nm and emission recorded from 300 to 450 nm at 150 nm/min. Slit widths of 5 and 10 nm were routinely used for the excitation and emission monochromators, respectively. The solvent-accessible surface area of *E. coli* butyryl-ACP (1L0I, [20] was calculated using UCSF Chimera software [27] with a probe radius of 1.4 Å.

Results and Discussion

Several biophysical methods have previously indicated that *V. harveyi* holo-rACP is largely unfolded in aqueous solution at neutral pH, likely due to electrostatic repulsive forces among its abundant acidic residues [23, 24]. Conversely, a folded conformation consisting of ~50% α-helix can be stabilized by minimizing these interactions with decreased pH, high ionic strength, or binding of divalent cations to specific acidic residues in the central Helix II of holo-ACP [23, 26]. Based on curve shape and mean residue ellipticity at 220 nm, circular dichroism indi-

cated that the apo form of rACP is also unfolded at neutral and basic pH, while the folded helical conformation is stabilized at mildly acidic pH values (pH 5) in 10 mM ammonium acetate, a buffer compatible with ESI-MS (Figure 1a).

Positive mode TurboIonspray ESI-MS of apo-rACP under similar solvent conditions produced a broad series of peaks with a CSD from 6^+ to 9^+ (maximum 8^+) (Figure 2a). Higher resolution ESI-MS analysis of rACP using an IonSpec 9.4-T Fourier transform-ion cyclotron resonance (FT-ICR) MS (not shown) revealed that each broad peak observed on the QTrap is actually a cluster of peaks arising from sodium adduct formation and variable oxidation of the lone methionine (Met-44) of rACP. Interestingly, no change in the CSD (average net charge 7.7) was observed over the range of pH 5 to 10 (Figure 2a), indicating that increased helical content of apo-rACP at low pH is not accompanied by a change in its solution conformation as assessed by ESI-MS. Similar ESI-MS results were obtained with holo-rACP, which contains the 4′-phosphopantetheine prosthetic group attached to a central serine residue (data not shown). Although isoelectric precipitation of rACP precluded measurement in aqueous buffer at lower pH values, positive mode ESI-MS spectra for apo-rACP in 50% acetonitrile, 0.1% formic acid were virtually identical to that shown in Figure 2a. CD indicated that apo-rACP adopts a helical conformation under these acidic organic conditions (Figure 1b).

Strategic placement of basic residues in ACP can influence its solution conformation; e.g., mutation of Ala-75 to His results in a more compact helical ACP at neutral pH due to charge neutralization [24]. Recently, we have shown that site-directed mutagenic neutralization of seven acidic divalent cation-binding residues at both ends of Helix II also increases helical content and decreases the hydrodynamic radius of ACP [26]. This ACP mutant (SA/SB) is expressed predominantly in the apo-form and cannot be further stabilized by divalent cation binding. As shown in Figure 1c, apo-SA/SB exhibited significantly greater helical content than apo-rACP at neutral pH and was only slightly unfolded even at pH 9.5. However, the CSD of this mutant exhibited only a modest change over this pH range, with average net charge decreasing from 8.0 at pH 9.5 to 7.6 at pH 4.4 (Figure 2b). Moreover, this profile was very similar to that of rACP, consistent with earlier observations that the CSD of a protein does not necessarily reflect its net charge in solution [15], which in this case would be considerably lower for SA/SB (total of 15 acidic residues) relative to rACP (22 acidic residues) at neutral and higher pH values.
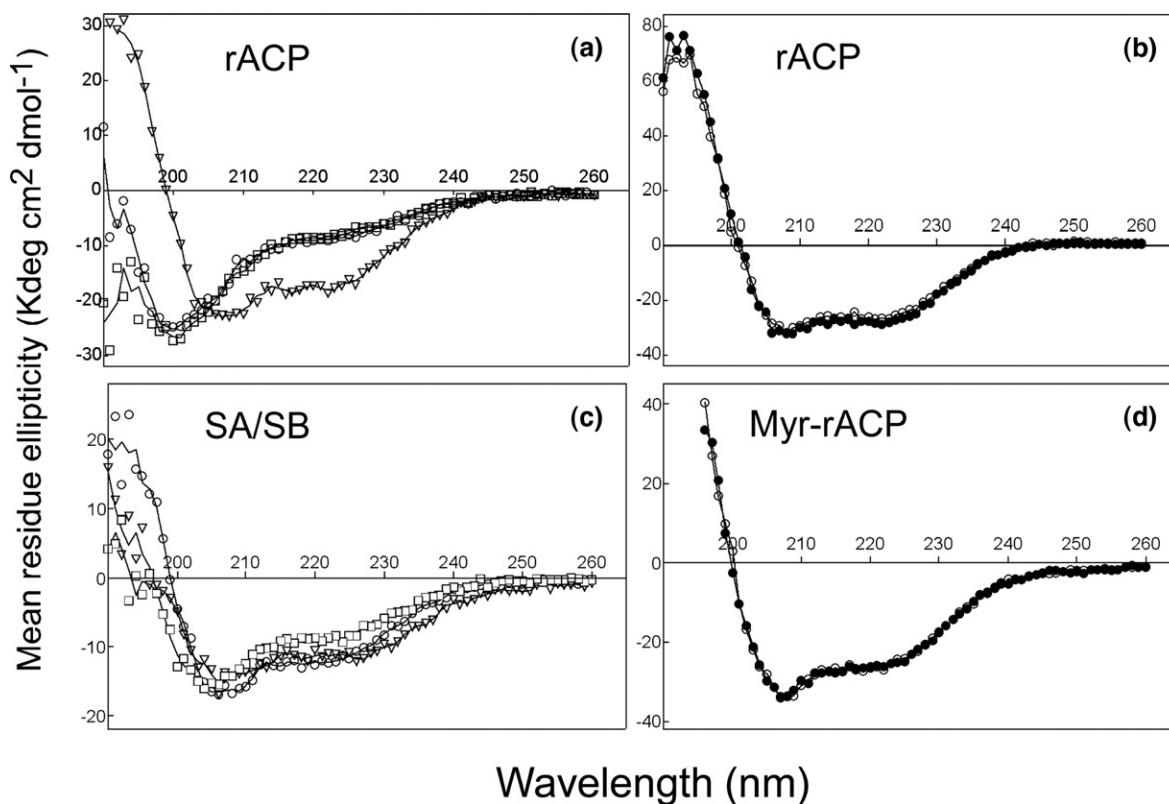

Figure 1. Circular dichroism of rACP and SA/SB mutant as a function of pH. (**a**) Apo-rACP in 10 mM ammonium acetate at pH 5.0 (inverted open triangle), 6.5 (O), and 9.2 (□). (**b**) Apo-rACP in 50% acetonitrile, 0.1% formic acid in the absence (O) and presence (●) of 2 mM MgCl₂. (**c**) Apo-SA/SB in 10 mM ammonium acetate at pH 4.4 (∇), 6.7 (O), and 9.5 (□). (**d**) Myristoyl-rACP in 10 mM ammonium acetate in the absence (O) and presence (●) of 2 mM MgCl₂.
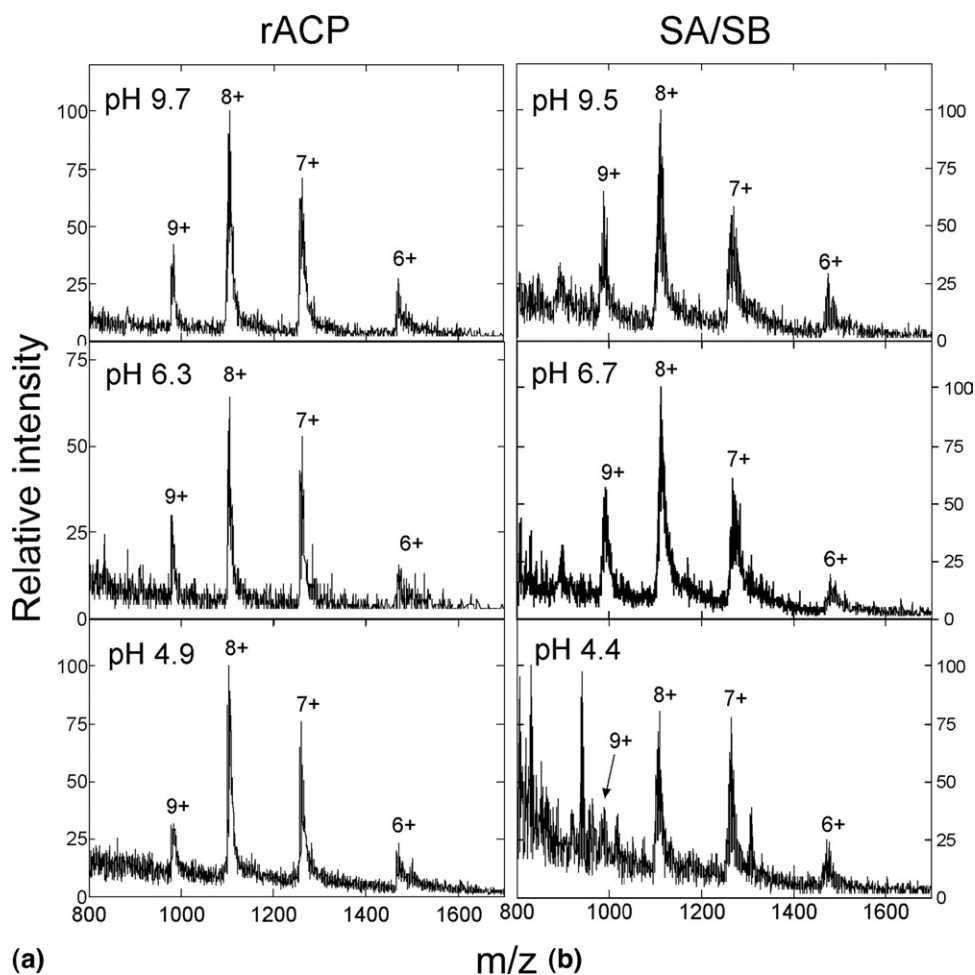
Figure 2. Positive mode TurboIonspray ESI-MS spectra of rACP and SA/SB mutant as a function of pH. Spectra of apo-proteins (1 μM) were recorded in 10 mM ammonium acetate at the indicated pH values as described in the text. The principal charge states are labeled above each peak.

As noted earlier, the accessibility of functional groups for ionization may not necessarily change during helix-coil transitions (i.e., changes in secondary structure), but is rather more closely related to tertiary structural alterations such as the burying of a segment of the polypeptide chain within a folded protein [13, 14]. To examine whether pH-induced changes in helical content of ACP reflect corresponding alterations in tertiary structure, we used a mutant of rACP in which leucine at position 46 in Helix II is replaced by the intrinsic fluorescence probe tryptophan. This residue is predicted to be buried in the hydrophobic core of folded ACP based on its known 3D structure [20, 21], and Mg^{2+}- or acylation-induced folding of the L46W mutant is accompanied by a pronounced blue shift in fluorescence emission as the Trp moves from an aqueous to a non-polar environment (Gong and Byers, manuscript in preparation). As shown in Figure 3b, decreasing the pH over the relatively narrow range of 6.5 to 5.5 also caused a blue shift of apo-L46W from a peak emission wavelength of 355 to 327 nm, an effect almost as large as that induced by Mg^{2+}. This correlated precisely with the low pH-induced increase in helical content (Figure 3a) and occurred over the same pH range as for rACP (Figure 1). Nevertheless, there was only a slight change in the CSD over this transition (Figure 4), with average net charge decreasing from 9.3 (pH 6.5) to 9.1 (pH 5.5). Note that a nanospray ion source was used for these experiments, resulting in a shift in the CSD (maximum 9^+) relative to TurboIonspray data presented earlier. However, this indicates that the insensitivity of the CSD to alterations in pH is not an artefact of a particular ESI-MS protocol.

In addition to reducing electrostatic repulsion by binding of divalent cations or lowering pH, attachment of a fatty acyl moiety to the phosphopantetheine thiol of holo-ACP can stabilize the folded helical conformation of *V. harveyi* ACP [23]. This stabilization occurs as the acyl chain is enclosed within the relatively hydrophobic interior of the three parallel α-helices of folded ACP, as indicated by both NMR [21] and X-ray crystallography [20]. As shown in Figure 5a, the CSD of myristoyl-ACP was very similar to that of apo-rACP (Figure 2a) at neutral pH (average net charge 7.6), although only the
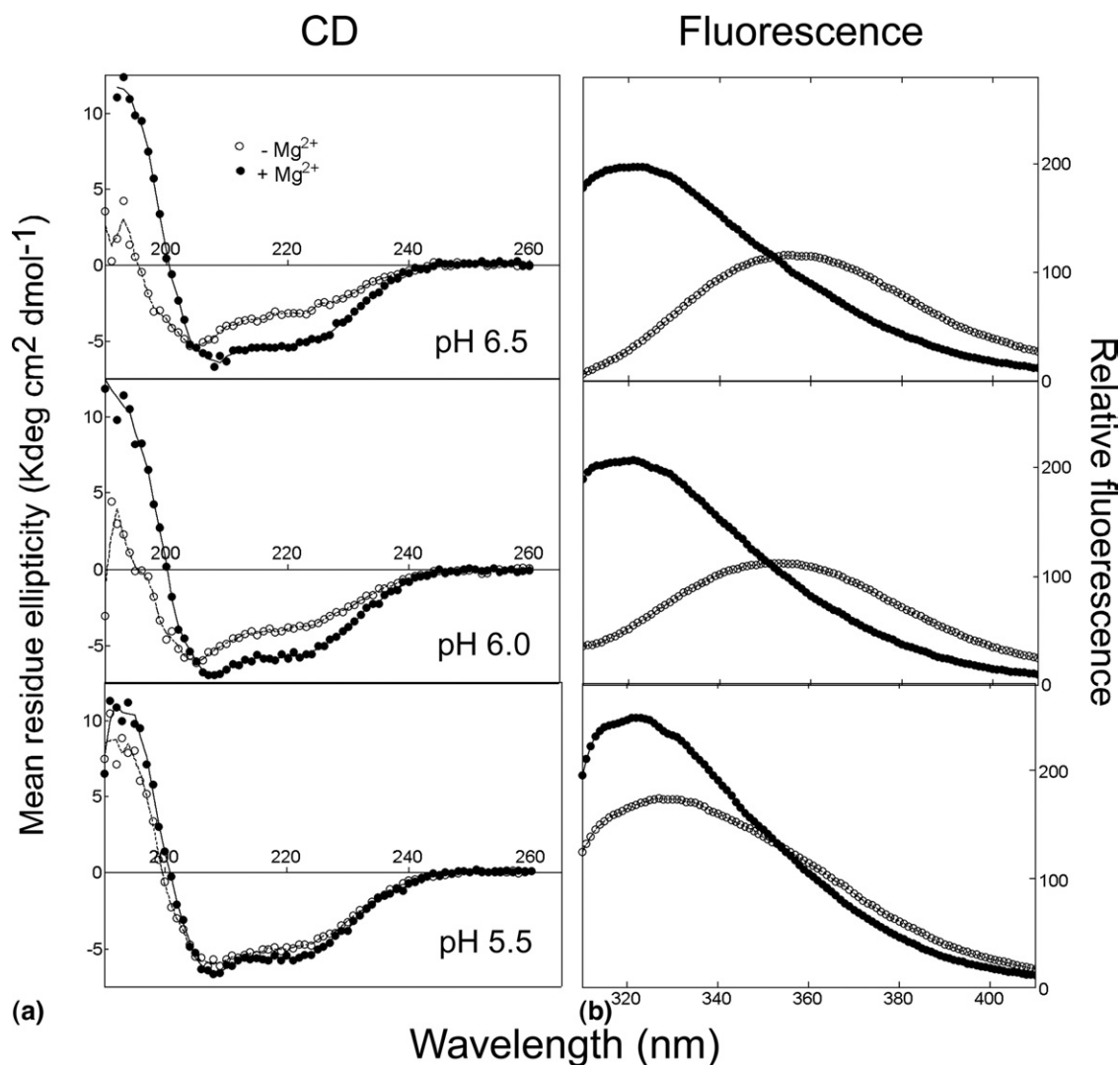
Figure 3. pH-induced secondary and tertiary structural alterations of ACP mutant apo-L46W. (**a**) CD and (**b**) fluorescence emission spectra of L46W (5 μM) in 10 mM ammonium acetate at the indicated pH values were obtained as described in the text, both before (○) and after (●) addition of 10 mM MgSO$_4$.

former would actually be in a folded helical conformation in solution under these conditions (Figure 1d).

While the CSD of neutral and basic proteins appears to better reflect their solution conformation using positive mode ESI-MS [15], acidic proteins are often analyzed in negative mode and conformational changes induced by calcium binding have been observed under these conditions [16, 17]. To investigate the effect of ionization polarity in our system, negative mode TurboIonspray ESI-MS spectra of both myristoyl-rACP (Figure 5b) and apo-rACP (Figure 5c) were obtained under identical conditions. Again, despite the distinct conformations of these two proteins in solution, only a modest difference in the CSD was observed, with average net charges of 8.4 and 8.7, respectively.

Overall, our results indicate that the CSD of ACP, in both positive and negative ion modes, is relatively insensitive to manipulations of its solution conforma-

tion by altering the pH, acidic amino acid content, or hydrophobic character of the protein. These results were not anticipated based on the considerable spectroscopic and hydrodynamic evidence, obtained here and in previous studies [22–24, 26, 28–30], that ACP folding involves transition to a more compact helical conformation. Unfolding of most proteins is accompanied by a pronounced shift from a narrow CSD of relatively low charge to a broader envelope of higher charge, often observed as bi- or multimodal distributions over the transition region [1, 14, 15]. Indeed, this typical behavior has been confirmed for the unfolding of cytochrome *c* at acidic pH [15] under our experimental conditions (Figure 6). We cannot rule out that discrete folded and unfolded states of ACP (as indicated by CD and fluorescence) have very similar CSD profiles due to comparable degrees of exposure of (de)protonation sites in the two conformations, but this is clearly at odds with most
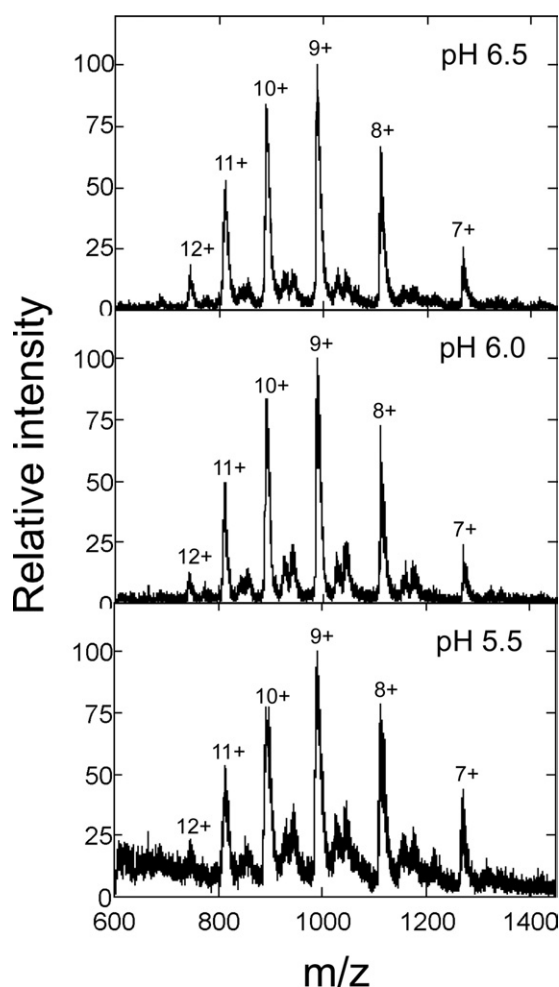
Figure 4. Positive mode nanospray ESI-MS spectra of ACP mutant L46W as a function of pH. Spectra of apo-proteins (5 μM) were recorded in 10 mM ammonium acetate at the indicated pH values as described in the text. The principal charge states are labeled above each peak.

proteins for which the CSD varies much more dramatically in the unfolded and folded states.

The unusual ESI-MS behavior of ACP is not likely due primarily to its acidic character, as it was not affected by replacement of several acidic residues in the SA/SB mutant. Moreover, pepsin (a highly acidic protein with 41 acidic and only four basic residues) exhibits a more typical 2- to 3-fold increase in average net charge upon unfolding [31] and a native CSD that reflects its solvent accessible surface area [10]. Likewise, the small size of ACP appears unlikely to be the sole basis of its unusual CSD properties, as ubiquitin (a protein of almost identical size to ACP) exhibits distinct and well resolved charge states as it undergoes conformational transitions [1].

A more plausible explanation is that the CSD profile of ACP is related to the particular properties of this flexible and dynamic protein. *E. coli* ACP in solution exhibits an ensemble of multiple folded conformations that exchange rapidly on the NMR time scale (<10 ms)

[32]; these transitions could provide accessibility to (de)protonation events during the electrospray ionization process. Indeed, ACP exhibits many of the features of natively unfolded or intrinsically unstructured proteins [33, 34], including a high ratio of charged to hydrophobic residues, anomalous migration on SDS-PAGE, and the ability to interact with a large number of partners in a coupled binding and folding process. Gel-filtration experiments have indicated that both *V. harveyi* and *E. coli* ACPs, which have 86% sequence identity but differ in helical content at neutral pH, have similar and abnormally high Stokes radii [22], indicating that they do not behave hydrodynamically as rigid globular proteins even under "native" conditions. It is also noteworthy that the average charge of ACP (at least 7.5+ in TurboIonspray experiments) is significantly larger than other proteins of similar size [10], suggesting a greater solvent exposed surface area than that
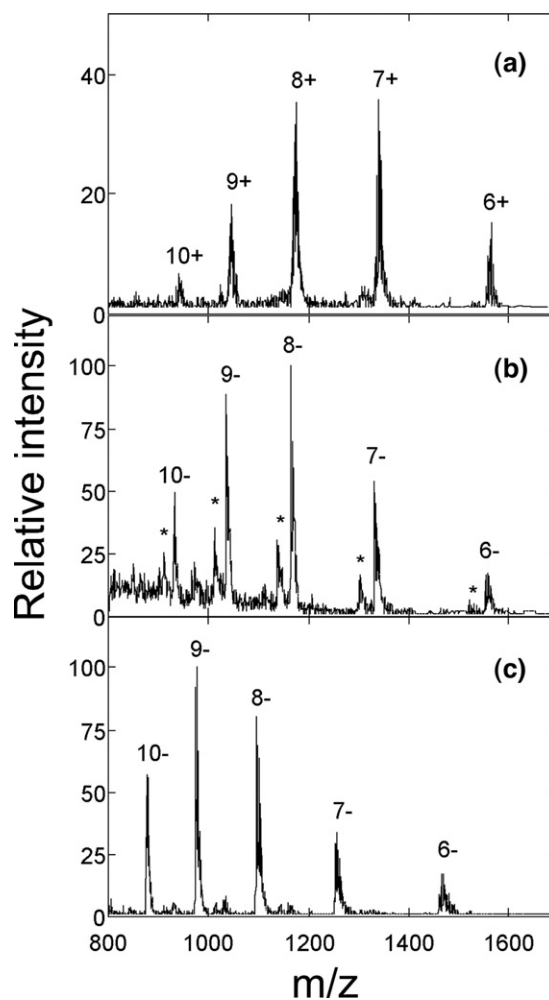

Figure 5. ESI-MS spectra of acyl-rACP in positive and negative ion modes. (**a**) Myristoyl-rACP in positive mode (pH 6.9). (**b**) Myristoyl-rACP in negative mode (pH 7.7). (**c**) Apo-rACP in negative mode (pH 7.7). All spectra were obtained in 10 mM ammonium acetate buffer. Principal charge states are labeled above each peak and the appearance of holo-ACP from de-acylation of acyl-ACP in (**b**) is indicated by an asterisk.
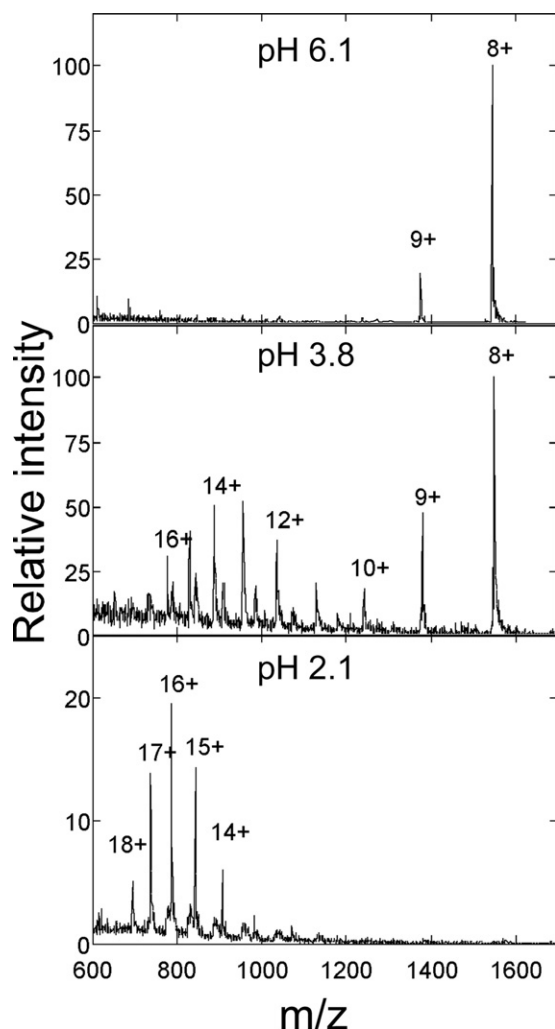
Figure 6. Positive mode ESI-MS spectra of cytochrome *c* as a function of pH. Spectra of cytochrome *c* (1 μM) in 5 mM ammonium acetate at the indicated pH values were recorded.

calculated from the crystal structure of butyryl-ACP (5245 Å^2). Thus, our data suggest that ACP could be at least partially unfolded or expanded during the electrospray process, resulting in a CSD that is relatively insensitive to conformational transitions observed by optical methods in solution.

Conclusions

We have shown that, unlike most proteins that have been previously investigated, the CSD of acyl carrier protein is not sensitive to major changes in its secondary and tertiary structure in solution. This was found to be the case in both positive and negative ESI modes, and occurred whether the folded ACP conformation was stabilized by electrostatic or hydrophobic interactions. The CSD of ACP also exhibited little correlation with the predicted solution charge of the protein and its average net charge was greater than expected from its calculated surface area. These results may reflect the particular dynamic properties of a "natively unfolded"

ACP, and further work with other natively unfolded proteins will be necessary to extend the generality of our conclusions. In the meantime, however, we suggest that caution should be exercised in the use of CSD to monitor conformational changes in proteins of this class.

References

1. Eyles, S. J.; Kaltashov, I. A. Methods to Study Protein Dynamics and Folding by Mass Spectrometry. *Methods* **2004,** *34,* 88–99.
2. Heck, A. J. R.; van den Heuvel, R. H. H. Investigation of Intact Protein Complexes by Mass Spectrometry. *Mass Spectrom. Rev.* **2004,** *23,* 368–389.
3. Konermann, L.; Simmons, D. A. Protein-Folding Kinetics and Mechanisms Studied by Pulse-Labeling and Mass Spectrometry. *Mass Spectrom. Rev.* **2003,** *22,* 1–26.
4. Maier, C. S.; Deinzer, M. L. Protein Conformations, Interactions, and H/D Exchange. *Methods Enzymol.* **2005,** *402,* 312–360.
5. Yan, X.; Watson, J.; Ho, P. S.; Deinzer, M. L. Mass Spectrometric Approaches Using Electrospray Ionization Charge States and Hydrogen-Deuterium Exchange for Determining Protein Structures and Their Conformational Changes. *Mol. Cell. Proteomics* **2004,** *3,* 10–23.
6. Chowdhury, S. K.; Katta, V.; Chait, B. T. Probing Conformational Changes in Proteins by Mass Spectrometry. *J. Am. Chem. Soc.* **1990,** *112,* 9012–9013.
7. Katta, V.; Chait, B. T. Conformational Changes in Proteins Probed by Hydrogen-Exchange Electrospray-Ionization Mass Spectrometry. *Rapid Commun. Mass Spectrom.* **1991,** *5,* 214–217.
8. Loo, J. A.; Edmonds, C. G.; Udseth, H. R.; Smith, R. D. Effect of Reducing Disulfide-Containing Proteins on Electrospray Ionization Mass Spectra. *Anal. Chem.* **1990,** *62,* 693–698.
9. Samalikova, M.; Grandori, R. Role of Opposite Charges in Protein Electrospray Ionization Mass Spectrometry. *J. Mass Spectrom.* **2003,** *38,* 941–947.
10. Kaltashov, I. A.; Mohimen, A. Estimates of Protein Surface Areas in Solution by Electrospray Ionization Mass Spectrometry. *Anal. Chem.* **2005,** *77,* 5370–5379.
11. Samalikova, M.; Matecko, I.; Muller, N.; Grandori, R. Interpreting Conformational Effects in Protein Nano-ESI-MS Spectra. *Anal. Bioanal. Chem.* **2004,** *378,* 1112–1123.
12. Vaidyanathan, S.; Kell, D. B.; Goodacre, R. Selective Detection of Proteins in Mixtures Using Electrospray Ionization Mass Spectrometry: Influence of Instrumental Settings and Implications for Proteomics. *Anal. Chem.* **2004,** *76,* 5024–5032.
13. Grandori, R.; Matecko, I.; Muller, N. Uncoupled Analysis of Secondary and Tertiary Protein Structure by Circular Dichroism and Electrospray Ionization Mass Spectrometry. *J. Mass Spectrom.* **2002,** *37,* 191–196.
14. Konermann, L.; Douglas, D. J. Acid-Induced Unfolding of Cytochrome *c* at Different Methanol Concentrations: Electrospray Ionization Mass Spectrometry Specifically Monitors Changes in the Tertiary Structure. *Biochemistry* **1997,** *36,* 12296–12302.
15. Konermann, L.; Douglas, D. J. Unfolding of Proteins Monitored by Electrospray Ionization Mass Spectrometry: A Comparison of Positive and Negative Ion Modes. *J. Am. Soc. Mass Spectrom.* **1998,** *9,* 1248–1254.
16. Watt, S. J.; Oakley, A.; Sheil, M. M.; Beck, J. L. Comparison of Negative and Positive Ion Electrospray Ionization Mass Spectra of Calmodulin and Its Complex with Trifluoperazine. *Rapid Commun. Mass Spectrom.* **2005,** *19,* 2123–2130.
17. Veenstra, T. D.; Johnson, K. L.; Tomlinson, A. J.; Naylor, S.; Kumar, R. Determination of Calcium-Binding Sites in Rat Brain Calbindin D28K by Electrospray Ionization Mass Spectrometry. *Biochemistry* **1997,** *36,* 3535–3542.
18. Johnson, K. A.; Verhagen, M. F. J. M.; Adams, M. W. W.; Amster, I. J. Differences Between Positive and Negative Ion Stabilities of Metal-Sulfur Cluster Proteins: An Electrospray Ionization Fourier Transform Ion Cyclotron Resonance Study. *Int. J. Mass Spectrom.* **2001,** *204,* 77–85.
19. White, S. W.; Zheng, J.; Zhang, Y. M.; Rock, C. O. The Structural Biology of Type II Fatty Acid Biosynthesis. *Annu. Rev. Biochem.* **2005,** *74,* 791–831.

20. Roujeinikova, A.; Baldock, C.; Simon, W. J.; Gilroy, J.; Baker, P. J.; Stuitje, A. R.; Rice, D. W.; Slabas, A. R.; Rafferty, J. B. X-Ray Crystallographic Studies on Butyryl-ACP Reveal Flexibility of the Structure Around a Putative Acyl Chain Binding Site. *Structure* (Camb.) **2002,** *10,* 825–835.

21. Zornetzer, G. A.; Fox, B. G.; Markely, J. L. Solution Structures of Spinach Acyl Carrier Protein with Decanoate and Stearate. *Biochemistry* **2006,** *45,* 5217–5227.

22. de la Roche, M. A.; Shen, Z.; Byers, D. M. Hydrodynamic Properties of *Vibrio harveyi* Acyl Carrier Protein and Its Fatty-Acylated Derivatives. *Arch. Biochem. Biophys.* **1997,** *344,* 159–164.

23. Flaman, A. S.; Chen, J. M.; Van Iderstine, S. C.; Byers, D. M. Site-Directed Mutagenesis of Acyl Carrier Protein (ACP) Reveals Amino Acid Residues Involved in ACP Structure and Acyl-ACP Synthetase activity. *J. Biol. Chem.* **2001,** *276,* 35934–35939.

24. Keating, M. M.; Gong, H.; Byers, D. M. Identification of a Key Residue in the Conformational Stability of Acyl Carrier Protein. *Biochim. Biophys. Acta* **2002,** *1601,* 208–214.

25. Shen, Z.; Fice, D.; Byers, D. M. Preparation of Fatty-Acylated Derivative of Acyl Carrier Protein Using *Vibrio harveyi* Acyl-ACP Synthetase. *Anal. Biochem.* **1992,** *204,* 34–39.

26. Gong, H.; Murphy, A.; McMaster, C. R.; Byers, D. M. Neutralization of Acidic Residues in Helix II Stabilizes the Folded Conformation of Acyl Carrier Protein and Variably Alters Its Function with Different Enzymes. *J. Biol. Chem.* **2007,** *282,* 4494–4503.

27. Pettersen, E. F.; Goddard, T. D.; Huang, C. C.; Couch, G. S.; Greenblatt, D. M.; Meng, E. C.; Ferrin, T. E. UCSF. Chimera—A Visualization System for Exploratory Research and Analysis. *J. Comput. Chem.* **2004,** *25,* 1605–1612.

28. Mayo, K. H.; Prestegard, J. H. Acyl Carrier Protein from *Escherichia coli.* Structural Characterization of Short-Chain Acylated Acyl Carrier Proteins by NMR. *Biochemistry* **1985,** *24,* 7834–7838.

29. Rock, C. O.; Cronan, J. E., Jr.; Armitage, I. M. Molecular Properties of Acyl Carrier Protein Derivatives. *J. Biol. Chem.* **1981,** *256,* 2669–2674.

30. Schulz, H. On the Structure-Function Relationship of Acyl Carrier Protein of *Escherichia coli. J. Biol. Chem.* **1975,** *250,* 2299–2304.

31. Abzalimov, R. R; Frimpong, A. K.; Kaltashov, I. A. Gas-Phase Processes and Measurements of Macromolecular Properties in Solution: On the Possibility of False Positive and False Negative Signals of Protein Unfolding. *Int. J. Mass Spectrom.* **2006,** *253,* 207–216.

32. Horvath, L. A.; Sturtevant, J. M.; Prestegard, J. H. Kinetics and Thermodynamics of Thermal Denaturation in Acyl Carrier Protein. *Protein Sci.* **1994,** *3,* 103–108.

33. Fink, A. L. Natively Unfolded Proteins. *Curr. Opin. Struct. Biol.* **2005,** *15,* 35–41.

34. Wright, P. E.; Dyson, H. J. Intrinsically Unstructured Proteins: Reassessing the Protein Structure-Function Paradigm. *J. Mol. Biol.* **1999,** *293,* 321–331.